Technetium-99m-Sestamibi Imaging with Nitrate Infusion to Detect Viable Hibernating Myocardium and Predict Postrevascularization Recovery

Gianni Bisi, Roberto Sciagrà, Giovanni M. Santoro, Vania Rossi and Pier Filippo Fazzini

Nuclear Medicine Unit, Department of Clinical Pathophysiology, University of Florence; and Division of Cardiology, Careggi Hospital; Florence, Italy

We tested the relationship of nitrate-induced changes in ^{99m}Tc-sestamibi perfusion tomography and first-pass radionuclide angiocardiography (FPRNA) with postrevascularization functional recovery of asynergic territories. **Methods:** Twenty-eight patients, all with prior infarction and left ventricular dysfunction, underwent two ^{99m}Tc-sestamibi rest studies: one under baseline conditions and the other with nitrate infusion. The baseline study was repeated after revascularization. Changes in global and regional perfusion and ventricular function were evaluated by perfusion tomography and FPRNA. Hibernating myocardium was identified by functional recovery in postrevascularization FPRNA. **Results:** Eleven patients and 31 segments in 19 coronary territories had functional recovery. Nitrate-induced FPRNA changes showed poor agreement with postrevascularization modifications: kappa = 0.24, ns, for the global and kappa = 0.32, $p < 0.01$ for regional function. The agreement between nitrate-induced and postrevascularization perfusion changes was good both considering the patients ($k = 0.57$, $p < 0.01$) and the abnormal coronary territories ($k = 0.63$, $p < 0.0005$). The agreement of nitrate-induced perfusion changes with postrevascularization functional outcome was excellent on a patient ($k = 1$, $p < 0.0005$), and coronary territory basis ($k = 0.82$, $p < 0.0005$). Conversely, the agreement between nitrate and postrevascularization FPRNA was poor: $k = 0.18$, ns. **Conclusion:** These data suggest that the nitrate-induced changes in ^{99m}Tc-sestamibi perfusion imaging are useful to detect hibernating myocardium which recovers its function after revascularization.

Key Words: first-pass radionuclide angiocardiography; hibernating myocardium; nitrates; technetium-99m-sestamibi

J Nucl Med 1995; 36:1994–2000

Hibernating myocardium recovers its function once coronary blood flow has been restored (*1,2*). The current approach to detect hibernating myocardium is based on the well-known relation between recognition of myocardial viability in asynergic areas and postrevascularization improvement. The most accurate way to identify hibernating myocardium is to demonstrate a perfusion/metabolism mismatch (preserved glucose uptake in severely hypoperfused tissue) by means of PET (*3*). Also recognition of ^{201}Tl uptake is considered to be a reliable method for detecting hibernating myocardium and, because of the limited availability of PET facilities, it is the most widely used approach (*4–7*).

According to most experimental data, ^{99m}Tc-sestamibi has favorable features for use as a viability tracer (*8–15*), but several human studies have shown that it may underestimate viable hibernating myocardium (*16–20*). The factors contributing to impaired ^{99m}Tc-sestamibi uptake in hibernating myocardium are probably flow dependency of tracer uptake (*10–12,14,21,22*), relatively low extraction fraction (*23,24*), rapid blood clearance (*8,10,21*) and the lack of major redistribution (*8,13,21*). A possible approach to overcome these limitations could be administering of ^{99m}Tc-sestamibi with a vasodilating stimulation to improve tracer delivery to hypoperfused areas and, hence, its uptake in viable tissue. Nitrate administration is known to increase coronary blood flow (*25–31*) and ^{201}Tl and ^{99m}Tc-teboroxime uptake in hypoperfused territories (*32–34*). Furthermore, nitrate administration in combination with functional imaging has predicted the postrevascularization outcome of asynergic territories (*35,36*).

This study was undertaken to verify whether acute administration of isosorbide dinitrate can improve ^{99m}Tc-sestamibi uptake in hypoperfused territories and to evaluate the value of this phenomenon in predicting the postrevascularization outcome of asynergic myocardium. We also performed first-pass radionuclide angiocardiography (FPRNA) during ^{99m}Tc-sestamibi injection under baseline conditions and with nitrates to compare the relative accuracy of perfusion and functional nitrate imaging in detecting hibernating myocardium and to evaluate the effect of nitrate-induced wall motion changes on ^{99m}Tc-sestamibi activity in asynergic areas.

Received Aug. 5, 1994; revision accepted May 15, 1995.

For correspondence or reprints contact: Roberto Sciagrà, Nuclear Medicine Unit, Department of Clinical Pathophysiology, University of Florence, Viale Morgagni 85, 50134 Florence, Italy.

METHODS

Patients

We studied 28 patients (24 men, 4 women; aged 42–71 yr, mean age 56.5 ± 8.5 yr), who had been scheduled for a coronary revascularization procedure because of low-threshold effort angina. Further inclusion criteria were: history of previous myocardial infarction dating back at least 3 mo, recent coronary angiography results, presence of left ventricular dysfunction (ejection fraction <50%) and a regional wall motion abnormality. Exclusion criteria were: history of unstable angina in the 3 mo immediately prior to the study, presence of heart disease other than coronary artery disease or history of previous revascularization procedures.

Study Protocol

All patients were studied after withdrawal of nitrate therapy for at least 48 hr; all other therapies were continued. Before revascularization, patients underwent ^{99m}Tc-sestamibi imaging under baseline conditions and with nitrate administration. The two studies were performed randomly, at least 24 hr apart, with the patients in stable clinical conditions. Each study included the collection of FPRNA during ^{99m}Tc-sestamibi injection for perfusion scintigraphy. For the nitrate study, 10 mg isosorbide dinitrate were diluted in 100 ml isotonic saline solution and infused over 20 min, while monitoring heart rate and blood pressure. Technetium-99m-sestamibi was injected as soon as systolic blood pressure dropped >20 mmHg or systolic blood pressure was <90 mmHg. Otherwise, the tracer was administered after 15 min of isosorbide dinitrate infusion. Rest FPRNA and ^{99m}Tc-sestamibi perfusion SPECT were repeated at least 3 mo after coronary bypass grafting, or at least 1 mo after coronary angioplasty, to assess the evolution of both global and regional left ventricular function and coronary perfusion. Informed consent to participate in the study was obtained from all patients. The study protocol had been previously approved by the ethics committee of our institution.

Coronary Angiography

Cardiac catheterization, including selective coronary angiography in multiple projections, was performed within 15 days before or after the scintigraphic study. The main epicardial coronary arteries were evaluated by two observers, who were blinded to the clinical and scintigraphic data. Each vessel was graded as having significant stenosis if the lesion restricted the lumen by ≥50%.

First-Pass Radionuclide Angiocardiography

FPRNA was acquired in the 30° right anterior oblique projection, with the patient supine, using a gamma camera equipped with a low-energy, all-purpose collimator. A 20% window was centered at the 140-keV photopeak of ^{99m}Tc. Twenty-five millicuries (925 MBq) ^{99m}Tc-sestamibi were injected into a saline-filled tubing extension ending with a three-way stop-cock and connected to an indwelling cannula, previously inserted into an antecubital vein of the right arm. The tracer bolus was then injected with forceful pushing with a booster flush of 20 ml saline solution (*37*). The bolus quality was controlled using the time-activity curve in a region of interest (ROI) drawn on the superior caval vein and defined acceptable when the FWHM was <1 sec. The study was acquired in frame mode (24 frames/sec) using a 2 × zoom factor and EKG gating to reconstruct the representative cardiac cycle. Left ventricular ejection fraction (LVEF) was calculated twice from the background-subtracted time-activity curve and the mean value was used for data analysis. The difference between the two measurements was never >2 ejection fraction units. A significant change in postrevascularization or in nitrate FPRNA was defined by modification of the global LVEF of ≥3 ejection fraction units compared with the baseline value. The choice of the threshold of 3 ejection fraction units was made taking into account the FPRNA reproducibility in our laboratory (*37*). For regional wall motion analysis, the left ventricular wall was divided into five segments and the motion of each segment was evaluated using the following scoring scheme: 0 = normokinesis, 1 = mild hypokinesis, 2 = severe hypokinesis, 3 = akinesis and 4 = dyskinesis (*37*). The anterior, antero-apical and apical segments were assigned to the territory of the left anterior descending artery and the inferior and infero-basal segments to that of the posterior descending artery. For each study, an image set, including left ventricular end-diastolic and end-systolic outlines, representative cycle cine movie display, regional ejection fraction images and Fourier amplitude images, was prepared and submitted blindly and independently to two experienced observers. In case of disagreement, which was registered in 25/420 (6%) assigned scores, the final score was given by consensus with the help of a third observer. According to the comparison between the nitrate or postrevascularization score and the related baseline value, each asynergic segment was classified as either improved (wall motion score decrease ≥1 grade) or unchanged. Similarly, a vascular territory was classified as improved if it included at least one segment with a wall motion score decrease ≥1 grade. Improvement in the postrevascularization study was also used to classify the territory as hibernating.

Technetium-99m-Sestamibi Scintigraphy

SPECT data were collected 60 min after ^{99m}Tc-sestamibi injection on a gamma camera equipped with an ultra-high resolution collimator, with a 20% window centered on the 140-keV photopeak of ^{99m}Tc. The gamma camera head rotated in step-and-shoot mode over a 180° arc, from the 45° right anterior oblique to the 45° left posterior oblique view, with 60 projections of 20 sec each. Images were collected with a 1.4× zoom factor and stored on 64 × 64 matrices. Image reconstruction was performed using back-projection without a preprocessing filter and with a Wiener reconstruction filter (dumping factor = 1, FWHM = 8 mm). No attenuation or scatter correction was used. The transaxial slices were realigned along the heart axis obtaining short-axis, vertical and horizontal long-axis slices.

For quantitative evaluation of the tomographic images, the short-axis slices from the first slice with apical activity to the last slice with activity at the base were used (*38*). Count profiles were generated by computer and plotted on a two-dimensional polar map for comparison with a gender-specific data base of rest ^{99m}Tc-sestamibi studies performed on normal control subjects (*39*). The lower limit of normal range was set at 2.5 s.d.s below the mean of the gender-specific control group (*38,39*). The extent of abnormally low uptake was first expressed as a percentage of the entire left ventricular wall. The quantitative polar map was then divided into three territories corresponding to distribution of the three coronary arteries. For each vascular territory, a separate analysis of tracer uptake was performed and the extent of the abnormality was expressed as a percentage of the single territory. A defect had to be >12% of the left anterior descending and the circumflex territories and >8% of the right coronary artery territory for clinical significance (*40*). The patient's total perfusion defect and significant regional defects in the nitrate and postrevascularization studies were compared with related baseline values. On the basis of this comparison, each patient study and territory defect was classified as either improved (extent decrease of >10% of the baseline value) or unchanged. For comparison with FPRNA data

TABLE 1
Patient Characteristics

Patients	28
Prior Infarct Sites	32
Anterior	15
Inferior	9
Anterior and Inferior	4
Coronary Angiography	
Three-vessel CAD	12
Two-vessel CAD	5
One-vessel CAD	11
Preoperative LVEF	36.2% ± 9.9% (range 16%–49%)

CAD = coronary artery disease; LVEF = left ventricular ejection fraction.

on a vascular territory basis, only the left anterior descending and the right coronary artery defects were considered and compared with anterior and posterior FPRNA territories, respectively.

Statistical Analysis

Data are expressed, when appropriate, as the mean ± s.d. Hemodynamic changes during the nitrate test were analyzed using one-way analysis of variance and the Bonferroni corrected t-test. Agreement between the nitrate-induced and postrevascularization changes was evaluated by chi square test with Yates correction and calculating the kappa value; values >0.75 represent excellent agreement, values between 0.40 and 0.75 show fair to good agreement and values <0.40 show poor agreement (*41*). Bonferroni correction was used for multiple comparisons. A probability value of $p < 0.05$ was significant.

RESULTS

General Findings

Table 1 summarizes the main preoperative findings of all patients. According to baseline FPRNA, there were 95 asynergic segments in 44 vascular territories (23 anterior, 21 posterior). Thirty-two were the site of a previous infarction; the remaining 12 included mostly asynergic segments contiguous to the infarcted ones. Nonetheless, the 12 noninfarcted asynergic areas were supplied by critically stenotic coronary arteries.

In the baseline perfusion study, 53 vascular territories (21 left anterior descending, 11 circumflex and 21 right coronary) showed a significant perfusion defect. All of them were asynergic. Therefore, 2 asynergic vascular territories had an apparently normal ^{99m}Tc-sestamibi uptake. Moreover, all normokinetic territories showed an apparently normal perfusion pattern.

Postrevascularization Findings

Complete revascularization of all stenosed major epicardial vessels was obtained using multiple bypass grafting in 18 patients and coronary angioplasty in 10. An increase ≥3 ejection fraction units in the LVEF was observed in 11 patients. The remaining 17 patients showed either a change <3 ejection fraction units or an ejection fraction decrease.

TABLE 2
Hemodynamic Response to the Nitrate Test

	Baseline	Nitrate	p
Heart rate (bpm)	66 ± 12	74 ± 12	0.05
Systolic BP (mmHg)	125 ± 17	105 ± 15	<0.0005
Diastolic BP (mmHg)	75 ± 10	68 ± 10	<0.05
Mean BP (mmHg)	92 ± 11	79 ± 10	<0.0005

BP = arterial blood pressure.

Thirty-one baseline asynergic segments had wall motion score improvement, whereas 64 were unchanged. Therefore, 19 FPRNA vascular territories (13 anterior and 6 posterior) showed significant postrevascularization wall motion recovery and were classified as hibernating. In the remaining 25 asynergic vascular territories, the total wall motion score remained unchanged.

In postrevascularization perfusion SPECT, 13 patients had significant decreases in total extent of perfusion defects and 15 had an unchanged value. In terms of vascular territories, 23 showed a perfusion defect decrease and 30 an unchanged defect extent.

Hemodynamic Findings During Nitrate Infusion

Technetium-99m-sestamibi was injected after 15 min into 20 patients; in another eight, the injection was anticipated as required by previously mentioned blood pressure criteria. Table 2 shows the hemodynamic parameters at the beginning of the infusion and at the moment of tracer injection. No patient suffered from adverse effects due to the nitrate infusion.

First-Pass Radionuclide Angiocardiography

Figures 1 and 2 show two examples of baseline and nitrate FPRNA images. Eleven patients had an ejection fraction increase, whereas the remaining 17 had unchanged ejection fractions. A low agreement ($k = 0.24$, ns) could be demonstrated between nitrate-induced and postrevascularization ejection fraction changes (Fig. 3). For segmental analysis, 44 had wall motion score improvement and 51 remained unchanged. Figure 3 shows the comparison between these changes and those observed in postrevascularization FPRNA. In this case, the agreement was quite poor, but significant ($k = 0.32$, $p < 0.01$). For vascular territories, 30 were improved and 14 unchanged, with low agreement with the postrevascularization data ($k = 0.18$, ns) (Fig. 4).

Perfusion Imaging

Two examples of baseline and nitrate myocardial scintigraphy are shown in Figures 1 and 2. A significant decrease in global extent of the perfusion defect was observed in 11 patients. The remaining 17 patients had unchanged global extent of perfusion defects. There was a fair agreement between nitrate-induced and postrevascularization changes ($k = 0.57$, $p < 0.01$, Fig. 5). Furthermore, nitrate-induced global perfusion defect changes correctly classified all patients as having significant ejection fraction increases or no

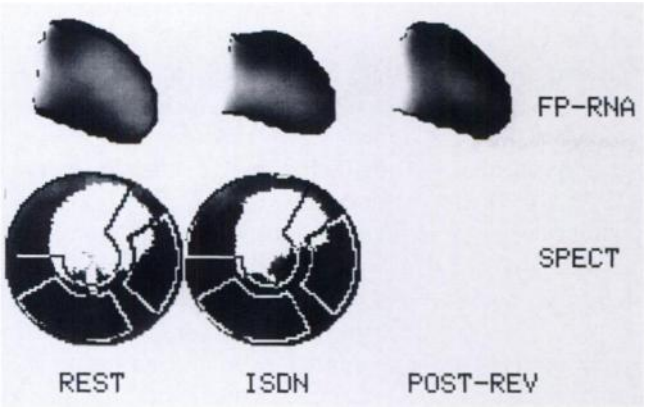

FIGURE 1. FPRNA and perfusion polar map (SPECT) of a patient with single-vessel CAD. Prerevascularization baseline images (REST) show antero-apical akinesia with a perfusion defect. The nitrate images (ISDN) show significant wall motion improvement and perfusion defect reduction. The postrevascularization (POST-REV) FPRNA confirms antero-apical functional recovery.

significant increase ($k = 1$, $p < 0.0005$) (Fig. 6). Of the 53 vascular territories with significant perfusion defects on baseline scintigraphy, 23 had a significant decrease in the defect extent with nitrates and 30 remained unchanged; there was good agreement with the postrevascularization changes ($k = 0.63$, $p < 0.0005$) (Fig. 5). When nitrate-induced perfusion changes in the 44 asynergic FPRNA territories were compared with the classified territories according to postrevascularization functional modifications, 18 of 19 hibernating territories were identified (16 by significant decreases in perfusion defect extent and 2 by completely normal perfusion in the baseline and nitrate studies). On the other hand, absence of hibernating myocardium was correctly predicted in 22/25 territories. Overall, there was an excellent agreement between nitrate-induced perfusion changes and presence or absence of postrevascularization functional recovery ($k = 0.82$, $p < 0.0005$) (Fig. 4).

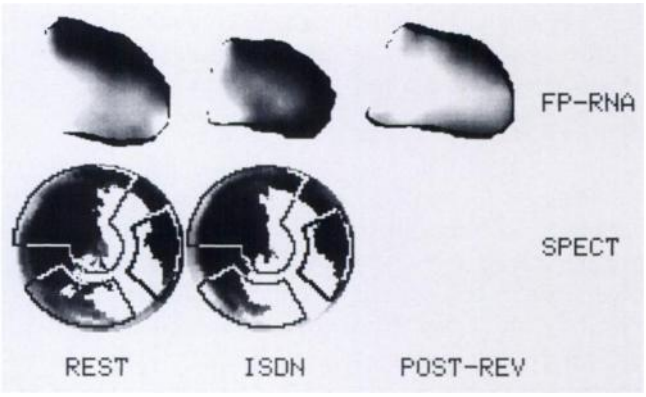

FIGURE 2. FPRNA and perfusion polar map (SPECT) of a patient with three-vessel CAD. Nitrate images demonstrate remarkable and diffuse improvement in wall motion pattern, but the perfusion defect does not appear modified. After revascularization, there is no functional recovery.

LVEF post-rev. vs. baseline

LVEF nitrate vs. baseline	Improved	Not improved	Total
Improved	6	5	11
Not improved	5	12	17
Total	11	17	28

Agreement = 64%
Kappa ± SE(K) = .24 ± .19

FPRNA post-rev. vs. baseline

FPRNA nitrate vs. baseline	Improved	Not improved	Total
Improved	22	22	44
Not improved	9	42	51
Total	31	64	95

Agreement = 67%
Kappa ± SE(K) = .32 ± .10

FIGURE 3. Agreement for global (top) and segmental (bottom) functional changes between postrevascularization (post-rev) and nitrate FPRNA. Both studies were compared with the prerevascularization baseline study. SE(K) = standard error of kappa.

DISCUSSION

Nitrates and Coronary Blood Flow

Organic nitrates are a mainstay of coronary artery disease therapy. Their anti-ischemic effect is mainly related to decreases in myocardial oxygen consumption, which are obtained by lowering of preload and afterload in the two ventricles (*42*). Recently, several reports have suggested that coronary vasodilation also plays an important role in anti-ischemic mechanisms of nitrates (*28,42,43*). Specifically, it has been hypothesized that nitrates dilate flow-

FPRNA post-rev. vs. baseline

FPRNA nitrate vs. baseline	Improved	Not improved	Total
Improved	15	15	30
Not improved	4	10	14
Total	19	25	44

Agreement = 57%
Kappa ± SE(K) = .18 ± .13

FPRNA post-rev. vs. baseline

SPECT nitrate vs. baseline	Improved	Not improved	Total
Improved	18	3	21
Not improved	1	22	23
Total	19	25	44

Agreement = 91%
Kappa ± SE(K) = .82 ± .15

FIGURE 4. Agreement between presence or absence of regional postrevascularization recovery and nitrate-induced functional (top) and perfusion (bottom) changes in comparable asynergic territories.

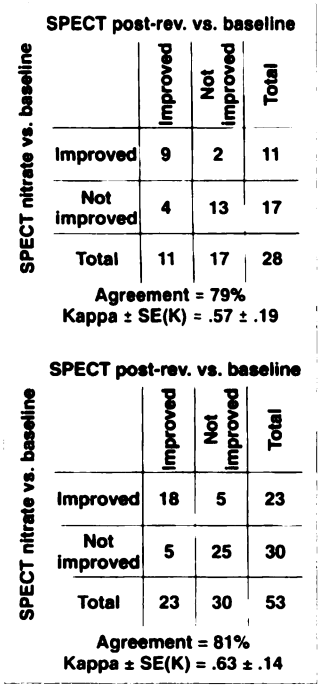

FIGURE 5. Agreement for global (top) and regional (bottom) perfusion changes between postrevascularization and nitrate tomography. Both studies were compared with the prerevascularization baseline study.

limiting obstructions in coronary arteries (*27,29*). Furthermore, there is the well-known vasodilating effect of nitrates on coronary collaterals (*26*), which also explains the improvement in ^{201}Tl uptake after nitroglycerin infusion in hypoperfused regions related to totally occluded coronary arteries but with well-developed collateral circulation (*31*). More recently, the increase in coronary blood flow is considered to be the cause of higher numbers of perfusion defects classified as reversible by ^{201}Tl reinjection imaging performed with nitrate administration (*32,33*).

Technetium-99m-Sestamibi and Myocardial Viability

These data suggest that acute administration of nitrates could be helpful overcoming the limitations of ^{99m}Tc-sestamibi imaging of viable hibernating myocardium. There is clear experimental evidence that ^{99m}Tc-sestamibi uptake and retention require the integrity of cell membrane and cellular viability (*9,14*) and that infarcted myocardium is unable to extract tracer (*12*). Tracer uptake in areas of reduced flow and partially impaired viability, however, seems more directly influenced by blood flow rather than cell death (*22*). This is not unexpected, considering the kinetics of ^{99m}Tc-sestamibi (*8,10–14,21–24*). Thus, it is not surprising that most data in humans suggest that rest ^{99m}Tc-sestamibi uptake may underestimate myocardial viability compared with other imaging methods such as PET or ^{201}Tl, particularly if qualitative image analysis is used (*17,18,20*). Moreover, functional recovery after revascularization was found in segments which, according to quantitative analysis of rest ^{99m}Tc-sestamibi uptake, had apparently necrotic tissue (*19*). The importance of reduced tracer delivery in producing low tracer uptake by viable, but hypoperfused regions is supported by the demonstration that the collection of ^{99m}Tc-sestamibi redistribution images reduces, at least partially, the underestimation of viability compared with ^{201}Tl imaging (*20*). On the other hand, territories with chronic hypoperfusion at rest may have coronary flow reserve that can be elicited by pharmacological stimulation (*46*).

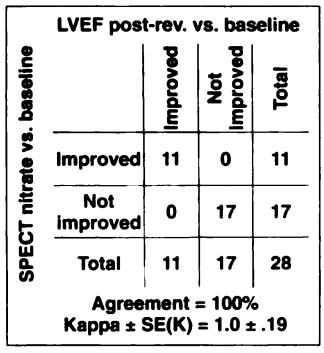

FIGURE 6. Agreement between presence or absence of postrevascularization LVEF improvement and nitrate-induced changes in global perfusion.

Nitrate Perfusion Imaging

In our patient population, most asynergic vascular territories had quantitative abnormal ^{99m}Tc-sestamibi uptake. In only 2 of 44 asynergic territories did apparently normal tracer uptake suggest the presence of hibernating myocardium. With nitrate administration, some patients and vascular territories had a clear decrease in global and regional uptake defect extent, respectively, whereas in the majority of cases unchanged perfusion was demonstrated. A comparison of these two different responses with the postrevascularization outcome confirms that nitrate ^{99m}Tc-sestamibi imaging is an effective method to detect viable hibernating myocardium. Nitrate-induced modifications in defect extent agreed with the perfusion changes observed after revascularization. All patients with a positive response to the nitrate test had significant improvement in global and regional ventricular function after revascularization. In the vascular territories, 86% of those with improvement on nitrate imaging, demonstrated functional recovery after revascularization. Conversely, 96% of the territories in which the presence of hibernating myocardium had been excluded did not improve after revascularization. In brief, nitrate ^{99m}Tc-sestamibi perfusion imaging accurately classified the postrevascularization outcome of all patients and 91% of the asynergic vascular territories.

Nitrate Functional Imaging

The possibility that long-lasting nitrate-induced wall motion changes produce apparent activity increase in the collected ^{99m}Tc-sestamibi perfusion images through partial volume effects (*45,47*), however, had to be considered. Reduction in cardiac loading and, possibly, the increase in collateral blood flow may explain the detection of contractile reserve in asynergic areas with acute nitrate administration (*30,35,36*). This finding has been correlated with a positive postrevascularization outcome (*35,36*). To evaluate this possible interaction and to test the hypothesis that functional nitrate imaging could be as effective as perfusion imaging to detect viable hibernating myocardium, we also

assessed acute functional changes induced by nitrate infusion by acquiring FPRNA during ^{99m}Tc-sestamibi injection. Although the nitrate FPRNA results agreed with those of perfusion imaging in some patients and vascular territories, there were also notable discrepancies. Specifically, a remarkably higher rate of positive responses to nitrate infusion was observed both on a patient and vascular territory basis. When the nitrate FPRNA results were compared with the postrevascularization outcome, however, most of these additional positive responses appeared to be false-positives because the patients and vascular territories involved did not show any functional recovery. This finding could be explained as a nonspecific consequence of decreases in cardiac pre- and afterload caused by peripheral hemodynamic actions of nitrates (*42,43*). On the other hand, the rate of false-negative responses to nitrate infusion was higher compared with perfusion imaging. Therefore, the value of nitrate functional imaging appeared significantly lower than perfusion scintigraphy for patient and vascular territory classifications. The remarkable disagreement between functional and perfusion modifications gives evidence against the hypothesis that increases in ^{99m}Tc-activity are mainly caused by nitrate-induced effects on wall motion and thickening, which could still be present during tomogram acquisition.

Study Limitations

These results must be evaluated with caution because of various study limitations. The patient sample size and the use of strict selection criteria must be considered. These are problems, however, common to most studies about hibernating myocardium. As for quantitative evaluation of tomographic images, we compared the count profiles of the baseline and nitrate studies with those of a database of normal subjects, which did not include patients with ventricular asynergia or dilatation. Theoretically, the difference in left ventricular shape, dimensions and wall thickness between normal subjects and patients with prior infarction could affect quantification of tracer activity. Nevertheless, this should not have influenced the reliability of the present study, since both the baseline and nitrate images were compared with the same normal reference and only the relative changes in tracer uptake were considered.

The limitations of FPRNA to evaluate regional ventricular function are well known, even though the use of functional images may reduce them (*47*). We tried to overcome the problem by using a simplified scheme which considered only the anterior and posterior vascular territories. More importantly, it must be remembered that the postrevascularization outcome was assessed by FPRNA. Therefore, no major errors in the evaluation of functional nitrate imaging compared to perfusion imaging should be ascribed to the use of FPRNA instead of other functional imaging techniques such as echocardiography. Naturally, the comparison between perfusion tomography and functional imaging was also complicated by the use of a planar technique such as FPRNA. The analysis based on two territories, however, should have diminished the inherent problems of this comparison.

CONCLUSION

This study demonstrates that acute nitrate infusion improves the capability of rest ^{99m}Tc-sestamibi perfusion imaging to detect viable hibernating myocardium, resulting in accurate prediction of postrevascularization outcome of both patients and vascular territories. In contrast, the acute effects of nitrate infusion on ventricular function, as assessed by FPRNA, appear to be significantly less reliable, particularly because of the nonspecific meaning of a positive response in terms of ventricular function. Further studies comparing nitrate ^{99m}Tc-sestamibi perfusion imaging with other currently used methods are warranted to define its clinical role in patients with chronic coronary artery disease and left ventricular dysfunction.

ACKNOWLEDGMENTS

Presented in part at the 41st Annual Meeting of the Society of Nuclear Medicine, Orlando, FL, June 1994.

REFERENCES

1. Braunwald E, Rutherford JD. Reversible left ventricular dysfunction: evidence for the "hibernating myocardium." *J Am Coll Cardiol* 1986;8:1467–1470.
2. Rahimtoola SH. The hibernating myocardium. *Am Heart J* 1988;117:211–221.
3. Tillisch JH, Brunken R, Marshall R, et al. Reversibility of cardiac wall motion abnormalities predicted by positron tomography. *N Engl J Med* 1986;314:884–888.
4. Iskandrian AS, Hakki A, Kane SA, et al. Rest and redistribution thallium-201 myocardial scintigraphy to predict improvement in left ventricular function after coronary artery bypass grafting. *Am J Cardiol* 1983;51:1312–1316.
5. Kiat H, Berman DS, Maddahi J, et al. Late reversibility of tomographic myocardial thallium-201 defects: an accurate marker of myocardial viability. *J Am Coll Cardiol* 1988;12:1456–1463.
6. Dilsizian V, Rocco TP, Freedman NM, Leon MB, Bonow RO. Enhanced detection of ischemic but viable myocardium by the reinjection of thallium after stress-redistribution imaging. *N Engl J Med* 1990;323:141–146.
7. Bonow RO, Dilsizian V, Cuocolo A, Bacharach SL. Identification of viable myocardium in patients with chronic coronary artery disease and left ventricular dysfunction. Comparison of thallium scintigraphy with reinjection and PET imaging with ^{18}F-fluorodeoxyglucose. *Circulation* 1991;83:26–37.
8. Okada RD, Glover D, Gaffney T, Williams S. Myocardial kinetics of technetium-99m-hexakis-2-methoxy-2-methylpropyl-isonitrile. *Circulation* 1988; 77:491–498.
9. Maublant JC, Gachon P, Moins N. Hexakis (2-methoxy isobutylisonitrile) technetium-99m and thallium-201 chloride: uptake and release in cultured myocardial cells. *J Nucl Med* 1988;29:48–54.
10. Li Q-S, Frank TL, Franceschi D, Wagner HN Jr, Becker LC. Technetium-99m methoxyisobutyl isonitrile (RP30) for quantification of myocardial ischemia and reperfusion in dogs. *J Nucl Med* 1988;29:1539–1548.
11. Sinusas AJ, Watson DD, Cannon JM Jr, Beller GA. Effect of ischemia and postischemic dysfunction on myocardial uptake of technetium-99m-labeled methoxyisobutyl isonitrile and thallium-201. *J Am Coll Cardiol* 1989;14:1785–1793.
12. Canby RC, Silber S, Pohost GM. Relations of the myocardial imaging agents ^{99m}Tc-MIBI and ^{201}Tl to myocardial blood flow in a canine model of myocardial ischemic insult. *Circulation* 1990;81:289–296.
13. Ll Q-S, Solot G, Frank TL, et al. Myocardial distribution of technetium-99m-methoxyisobutyl isonitrile (sestamibi). *J Nucl Med* 1990;31:1069–1076.
14. Sinusas AJ, Trautman KA, Bergin JD, et al. Quantification of area at risk during coronary occlusion and degree of myocardial salvage after reperfusion with technetium-99m methoxyisobutyl isonitrile. *Circulation* 1990;82: 1424–1437.
15. Freeman I, Grunwald AM, Hoory S, Bodenheimer MM. Effect of coronary

occlusion and myocardial viability on myocardial activity of technetium-99m-sestamibi. *J Nucl Med* 1991;32:292–298.
16. Rocco TP, Dilsizian V, Strauss HW, Boucher CA. Technetium-99m isonitrile myocardial uptake at rest. II. Relation to clinical markers of potential viability. *J Am Coll Cardiol* 1989;14:1678–1684.
17. Altenhoefer C, Kaiser H-J, Dörr R, et al. Fluorine-18 deoxyglucose PET for the assessment of viable myocardium in perfusion defects in ^{99m}Tc-MIBI SPECT: a comparative study in patients with coronary artery disease. *Eur J Nucl Med* 1992;19:334–342.
18. Cuocolo A, Pace L, Ricciardelli B, Chiariello M, Trimarco B, Salvatore M. Identification of viable myocardium in patients with chronic coronary artery disease: comparison of thallium-201 scintigraphy with reinjection and technetium-99m-methoxyisobutyl isonitrile. *J Nucl Med* 1992;33:505–511.
19. Marzullo P, Sambuceti G, Parodi O. The role of sestamibi scintigraphy in the radioisotopic assessment of myocardial viability. *J Nucl Med* 1992;33:1925–1930.
20. Dilsizian V, Arrighi JA, Diodati JG, et al. Myocardial viability in patients with chronic coronary artery disease. Comparison of ^{99m}Tc-sestamibi with thallium reinjection and [^{18}F]fluorodeoxyglucose. *Circulation* 1994;89:578–587.
21. Wackers F, Berman D, Maddahi J, et al. Technetium-99m hexakis 2-methoxyisobutyl isonitrile: human biodistribution, dosimetry, safety and preliminary comparison to thallium-201 for myocardial perfusion imaging. *J Nucl Med* 1989;30:301–311.
22. Mehry Y, Latour J-G, Arsenault A, Rousseau G. Effect of coronary reperfusion on technetium-99m methoxyisobutylisonitrile uptake by viable and necrotic myocardium in the dog. *Eur J Nucl Med* 1992;19:503–510.
23. Leppo JA, Meerdink DJ. Comparison of the myocardial uptake of a technetium-labeled isonitrile analogue and thallium. *Circ Res* 1989;65:632–639.
24. Marshall RC, Leidholdt EM Jr, Zhang D-Y, et al. Technetium-99m hexakis 2-methoxy-2-isobutyl isonitrile and thallium-201 extraction, washout and retention at varying coronary flow rates in rabbit heart. *Circulation* 1990;82:998–1007.
25. Cohn PF, Maddox D, Holman BL, Markis JE, Adams DF, See JR. Effect of sublingually administered nitroglycerin on regional myocardial blood flow in patients with coronary artery disease. *Am J Cardiol* 1977;39:672–678.
26. Cohen MV, Sonnenblick EH, Kirk ES. Comparative effects of nitroglycerin and isosorbide dinitrate on coronary collateral vessels and ischemic myocardium in dogs. *Am J Cardiol* 1976;37:244–249.
27. Brown BG, Bolson EL, Petersen RB, Pierce CD, Dodge HT. The mechanism of nitroglycerin action: stenosis vasodilation as a major component of the drug response. *Circulation* 1981;64:1089–1097.
28. Feldman RI, Conti CR. Relief of myocardial ischemia with nitroglycerin: what is the mechanism? *Circulation* 1981;64:1098–1100.
29. Brown BG. Response of normal and diseased epicardial coronary arteries to vasoactive drugs: quantitative arteriographic studies. *Am J Cardiol* 1985;56:23E–29E.
30. Fujita M, Yamanishi K, Hirai T, et al. Significance of collateral circulation in reversible left ventricular asynergy by nitroglycerin in patients with relatively recent myocardial infarction. *Am Heart J* 1990;120:521–528.
31. Aoki M, Sakai K, Koyanagi S, Takeshita A, Nakamura M. Effect of nitroglycerin on coronary collateral function during exercise evaluated by quantitative analysis of thallium-201 SPECT. *Am Heart J* 1991;121:1361.
32. Medrano R, Mahmarian JJ, Verani MS. Nitroglycerin before reinjection of thallium-201 enhances detection of reversible hypoperfusion via collateral blood flow: a randomized, double blind, parallel, placebo-controlled trial [Abstract]. *J Am Coll Cardiol* 1993;21:221A.
33. He Z-X, Darcourt J, Guigner A, et al. Nitrates improve detection of ischemic but viable myocardium by thallium-201 reinjection SPECT. *J Nucl Med* 1993;34:1472–1477.
34. Bisi G, Sciagrà R, Santoro GM, Zerauschek F, Fazzini PF. Sublingual isosorbide dinitrate to improve ^{99m}Tc-teboroxime perfusion defect reversibility. *J Nucl Med* 1994;35:1274–1278.
35. Helfant RH, Pine R, Meister SG, Feldman MS, Trout RG, Banka VS. Nitroglycerin to unmask reversible asynergy. Correlation with post coronary bypass ventriculography. *Circulation* 1974;50:108–113.
36. Chesebro JH, Ritman EL, Frye RL, et al. Regional myocardial wall thickening response to nitroglycerin. A predictor of myocardial response to aortocoronary bypass surgery. *Circulation* 1978;57:952–957.
37. Sciagrà R, Bisi G, Santoro GM, Briganti V, Leoncini M, Fazzini PF. Evaluation of coronary artery disease extent and severity using ^{99m}Tc-sestamibi first pass and perfusion imaging in combination with dipyridamole infusion. *J Nucl Med* 1994;35:1254–1264.
38. DePasquale EE, Nody AC, DePuey EC, et al. Quantitative rotational thallium-201 tomography for identifying and localizing coronary artery disease. *Circulation* 1988;77:316–327.
39. Galli M, Marcassa C, Bolli R, et al. Spontaneous delayed recovery of perfusion and contraction after the first 5 weeks after anterior infarction. Evidence for the presence of hibernating myocardium in the infarcted area. *Circulation* 1994;90:1386–1397.
40. Maddahi J, Van Train K, Prigent F, et al. Quantitative single photon emission computed thallium-201 tomography for detection and localization of coronary artery disease: optimization and prospective validation of a new technique. *J Am Coll Cardiol* 1989;14:1689–1699.
41. Fleiss JL. The measurement of interrater agreement. In: Fleiss JL. *Statistical methods for rates and proportions*, 2nd ed. New York: Wiley; 1981:212–236.
42. Abrams J. Hemodynamic effects of nitroglycerin and long nitrates. *Am Heart J* 1985;110:216–224.
43. Abrams J. Mechanisms of action of the organic nitrates in the treatment of myocardial ischemia. *Am J Cardiol* 1992;70:30B–42B.
44. Parodi O, Sambuceti G, Roghi A, et al. Residual coronary reserve despite decreased resting blood flow in patients with critical coronary lesions. A study by technetium-99m human albumin microsphere myocardial scintigraphy. *Circulation* 1993;87:330–344.
45. Hoffman EJ, Huang SC, Phelps ME. Quantification in PET. I. Effects of object size. *J Comput Assist Tomogr* 1979;3:299–308.
46. Sinusas AJ, Shi Q, Vitols PJ, et al. Impact of regional ventricular function, geometry, and dobutamine stress on quantitative ^{99m}Tc-sestamibi defect size. *Circulation* 1993;88:2224–2234.
47. Bodenheimer MM, Banka VS, Fooshee CM, Hermann GA, Helfant RH. Comparison of wall motion and regional ejection fraction at rest and during exercise: concise communication. *J Nucl Med* 1979;20:724–732.